

## SMALL-DIAMETER ROTATING COILS FOR FIELD QUALITY MEASUREMENTS IN QUADRUPOLE MAGNETS

*H. Braun*<sup>2</sup>, *M. Buzio*<sup>1</sup>, *R. Deckardt*<sup>2</sup>, *O. Dunkel*<sup>1</sup>, *R. Felder*<sup>2</sup>, *L. Fiscarelli*<sup>1</sup>, *R. Ganter*<sup>2</sup>,  
*S. Kasaei*<sup>1</sup>, *F. Löhle*<sup>2</sup>, *S. Sanfilippo*<sup>2</sup>, *G. Severino*<sup>1</sup>, *V. Vrankovic*<sup>2</sup> and *L. Walckiers*<sup>1</sup>

<sup>1</sup>CERN, 1211 Geneva, Switzerland

<sup>2</sup>Paul Scherrer Institut, 5232 Villigen, Switzerland

**Abstract** – Two rotating coil shafts with a challenging small diameter of 8 and 19 mm, originally developed at CERN for the measurement of linear accelerator magnets, have been used to quantify the magnetic field strength, the harmonic content and the field direction of series quadrupoles for the Swiss Free Electron Laser in construction at the Paul Scherrer Institute. In this paper, we describe the design and construction of these coils, the procedure used for their calibration, and the results obtained on the magnets tested so far. We focus especially on the manufacturing and calibration difficulties related to the very small diameter of these coils, which makes it challenging to obtain relative errors at the level of a few  $10^{-4}$  as it is commonly required by accelerator beam optics. The last part of the paper is dedicated to a selection of measurement results obtained on Swiss Free Electron Laser quadrupoles to illustrate the performance of the two types of coils on series measurements.

**Keywords** **harmonic coils, particle accelerator, small aperture quadrupole magnets, field quality**

### 1. INTRODUCTION

#### 1.1. Quadrupole magnets for particle accelerators

High-energy particle accelerators and new generation of light sources such as the Swiss Free Electron Laser (SwissFEL) [1], currently in construction at the Paul Scherrer Institute (Villigen, Switzerland), require in general quadrupole magnets acting as optical lenses to focus the beam [2]. The average magnetic field created by accelerator magnets can be described by the complex harmonic expansion (1):

$$B_y + iB_x = \sum_{n=1}^{\infty} \underbrace{(B_n + iA_n)}_{c_n} \left( \frac{x+iy}{r_{ref}} \right)^n \quad (1)$$

where  $x, y$  are transversal coordinates,  $B_n$  and  $A_n$  represent respectively the so-called normal and skew harmonic field components and  $r_{ref}$  is a reference radius comparable with

the beam size [3]. The field components are in general weakly non-linear functions of the excitation current level and history, due to saturation and hysteresis effects in the iron yoke of the electromagnets. In the case of a quadrupole magnet the  $n=1$  (dipole) field components are zero and therefore the field vanishes along the magnet axis,  $z=0$ , which coincides with the nominal (ideal) beam trajectory. The focusing effect arises from the dominant  $n=2$  terms, which represent a constant field gradient  $G = \sqrt{B_2^2 + A_2^2}/r_{ref}$  and hence a Lorentz force that bends the trajectory of each particle in proportion to its offset with respect to the axis. Harmonic terms of order  $n \geq 3$  represent field errors which are typically of the order of  $10^{-4} \sim 10^{-3}$  with respect to the main quadrupole term.

Accelerator magnets have to be magnetically tested for qualification and the measurement results are used for the operation of the machine. In the case of quadrupoles, main test results include the integrated gradient  $\int G dl$ , the integrated field direction i.e. the electrical phase of the main harmonic  $\alpha = -\frac{1}{2} \tan^{-1} A_2/B_2$  and the transversal offset of the magnetic axis with respect to a given set of mechanical or optical references on the magnet yoke. Field errors are usually represented in terms of harmonic coefficients, normalized with respect to the main component and expressed in units of  $10^{-4}$ :

$$c_n = b_n + ia_n = 10^4 \frac{B_n + iA_n}{\|B_2 + iA_2\|} \quad (2)$$

This representation is ideally suited for synchrotrons, where the magnitude of the normalized field errors can be directly related to beam resonances and instabilities. Other representations based on the degree of uniformity of the field (or one of its derivatives) within the region where the beam passes can also be used.

#### 1.2. SwissFEL quadrupole tests

This paper reports on the series measurements of the small-aperture quadrupole electromagnets that will equip the X-ray free electron laser SwissFEL. A total number of 162 quadrupoles, featuring apertures of  $\varnothing 22$  mm and  $\varnothing 12$  mm

were designed and fabricated, and have to be magnetically qualified before the end of 2015 at the Paul Scherrer Institute. These quadrupoles will be installed in the low emittance injector, the linac and in the undulator beam lines, which have the function to provide the initial acceleration of the beam and to generate synchrotron light respectively. In Table I we summarize the parameters of the three types of quadrupoles called QFF, QFD and QFM. The QFF and QFD have integrated steerers wound around the quadrupole yoke, i.e. an additional set of coils able to produce horizontal and vertical dipole field components which have the function to apply systematic correction to the beam trajectory. More details on the quadrupole design and construction can be found in [4].

TABLE I. SPECIFICATIONS OF SWISSFEL QUADRUPOLES

Quadrupole type	QFF	QFD	QFM
Number	24	120	18
Cooling mode	air	air	water
Aperture diameter (mm)	12	22	22
Iron length (mm)	80	150	300
Total Magnet length (mm)	130	204	435
Weight (kg)	32	80	180
Nominal gradient $G_0$ (T/m)	50	25	50
Pole Tip Field (T)	0.3	0.275	0.55
Integrated Field Gradient uniformity (% rms)	<0.5	<0.5	<0.5
Harmonic/main field ratio (%)	<0.5	<0.5	<0.5
Maximum current (A)	10	10	50

The main challenge posed by testing these quadrupoles is represented by the small diameter of their aperture. The series-measurements are currently being carried out at PSI with a  $\varnothing 8$  mm and a  $\varnothing 19$  mm rotating coil system, originally developed at CERN for similar applications. The  $\varnothing 19$  mm system (Fig. 1), based on a monolithic coil shaft, was designed to test permanent-magnet and fast pulsed quadrupoles for the Linac4 injector currently being built at CERN and is described in detail in [5, 6]; the  $\varnothing 8$  mm system (Fig. 2), based on a coil array built with a multi-layer printed-circuit board (PCB) assembly, was developed to measure prototype quadrupoles for the CLIC linear collider project and is described in [7]. Both shafts include a similar configuration of three rectangular coils stacked on top of each other; the outermost coil is normally used to measure the main field component, while all three are combined in series to cancel out the dipole and quadrupole signals in order to get field harmonics with higher accuracy (“harmonic bucking”).

The structure of the paper is as follows. In Section 2, we summarize first briefly the theory of rotating coil measurements and the relative calibration techniques. In Sections 3 and 4, we discuss in detail the results of the calibrations and the cross-checks done at CERN and at PSI of the two rotating coil systems, focusing on the uncertainty of the results in the case of small-aperture magnets. Some results obtained on the series SwissFEL quadrupoles are presented in Section 5 to illustrate the performance of the

rotating coils. Finally, our conclusions are outlined in Section 6.



Fig. 1 -  $\varnothing 19$  mm rotating coil shaft mounted on the test bench used for the in-situ calibration. The translation stage shown is used to displace the reference magnet precisely.



Fig. 2 – Detail of three  $\varnothing 8$  mm rotating coil shafts

## 2. HARMONIC COIL METHOD FOR SMALL APERTURE MAGNETS

### 2.1. Harmonic coil method

The harmonic (rotating) coil is the instrument of choice, at CERN and elsewhere, to carry out high accuracy measurements of the integral field quality of accelerator magnets [8], in particular in the case of series measurements where test duration is a critical parameter. Compared to popular alternatives such as scanners based on commercial Hall-effect probes, for example, this method admittedly requires more specialized (and expensive) fabrication and calibration techniques. However, not only it is naturally better suited to integral field measurements but, as we will discuss more in detail below, it yields intrinsically higher accuracy for those quantities defined as ratios of harmonics, such as the normalized field errors.

The magnetic flux  $\Phi$  linked by the coil as a function of the trigonometric rotation angle  $\theta$  can be expressed by the Fourier series (see Fig. 3):

$$\Phi(\theta) = \Re \sum_{n=1}^{\infty} \frac{\kappa_n}{r_{ref}^{n-1}} C_n e^{in\theta} \quad (3)$$

where the so-called sensitivity coefficients  $\kappa_n$  are complex functions of the geometry of the coil. In our case the shafts are built with a tangential coil geometry (winding plane normal to the rotation radius). The coefficients are expressed in (4):

$$\kappa_n = \frac{N_T L_c}{n} \left[ \left( R_c + i \frac{w}{2} \right)^n - \left( R_c - i \frac{w}{2} \right)^n \right] \quad (4)$$

where  $R_c$  is the radius in the center of the coil winding,  $L_c$  is the coil length,  $N_T$  is the number of turns and  $w$  represents the effective coil width, defined by ignoring the finite size of the winding. In this representation, the total (effective) area of the coil is given by  $A_c = N_T L_c w$ .

Knowledge of these four geometrical parameters allows calculation of all sensitivity coefficients and the inversion of (3) to derive the field harmonic coefficients  $C_n$  from the respective DFT components  $\Psi_n$  of the flux:

$$C_n = \frac{2}{N} \frac{r_{ref}^{n-1}}{\kappa_n} \Psi_n \quad (5)$$

where  $N$  represents the number of sampling points of the flux over a full coil turn.

In general, we can consider the number of turns as a parameter known from the coil design phase. Conversely,  $L_c$  can be regarded as a mere reference parameter: the field components computed from (5) are in fact averages over the coil length, the precise value of which does not change the value of the integrated components  $C_n L_c$  (i.e. the quantity of interest for beam optics). For practical purposes, the value of  $L_c$  can either be taken as the nominal design parameter or be measured with simple mechanical means within a relaxed tolerance, typically a few 0.1 mm. Thus, calibration of the coil geometry is reduced essentially to the precise measurement of  $R_c$  and  $w_c$  (or equivalently  $A_c$ ). These quantities can hardly be obtained using mechanical or optical instrumentation and are customarily derived from magnetic measurements in well-known reference dipoles and quadrupoles, as explained in detail in [9].

When the coil is longer than the extent of the field being measured, the longitudinal distribution of the geometrical imperfections of the winding can have an impact on the accuracy of the measurement. In this case calibration of the average values of  $R_c$  and  $A_c$ , suitably weighted with the longitudinal profile of the magnetic field, can be carried out inside a magnet taken from the series to be tested, measured preliminarily with an already-calibrated instrument ad set aside as a reference. The moving wire and the Hall probe methods are well suited for this reference measurement, each one having a specific advantage: the moving wire provides directly integral results with extremely high precision, given by the precision of the translation stages (typical better than one micron); Hall probes give absolute measurements and are compatible with small magnets and low fields. This technique, referred to as “in-situ calibration”, has been used in the present application and explained in [10].

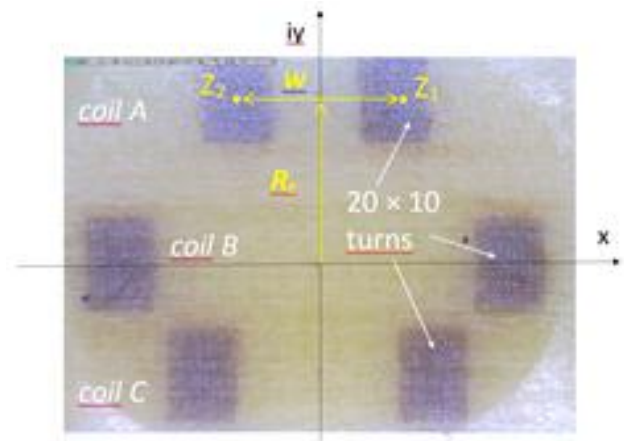


Fig. 3 – Geometry of the cross-section  $\varnothing 8$  mm PCB coil shaft, showing three parallel coils stacked on top of each other. Each winding is approximated by filaments at  $z=z_1$  and  $z=z_2$ .

## 2.2. Measurement uncertainty

The accuracy of harmonic coil measurements degrades noticeably for small-diameter aperture magnets. In general, the small scale implies that static and dynamic deformations, vibrations, alignment and temperature drifts are more difficult to control. Mechanical manufacturing tolerances, in particular, have the highest impact. Let us consider, for the sake of simplicity, the case of a tangential coil of finite surface area but vanishing  $w/R_c$  ratio, in which we can approximate (4) as:

$$\|\kappa_n\| \approx \frac{A_c R_c^{n-1}}{n} \quad (6)$$

By propagating errors in (5) we can easily derive an expression linking the relative uncertainties  $\sigma$  in the sensitivity coefficients to the relative uncertainties of the geometrical parameters:

$$\left( \frac{\sigma_{\|\kappa_n\|}}{\|\kappa_n\|} \right)^2 = \left( \frac{\sigma_{A_c}}{A_c} \right)^2 + (n-1)^2 \left( \frac{\sigma_{R_c}}{R_c} \right)^2 \quad (7)$$

In (7), the quadratic summation is necessary due to the random nature of the uncertainties (we shall lump systematic, but unknown, uncertainties together with the truly random errors, as recommended by ISO [11]). The term linked to the coil radius is, typically, the dominant one. The calibration of the equivalent coil areas, which is carried out in very precisely NMR-mapped reference dipole magnet, provides relative uncertainties of the order of a few  $10^{-4}$ . On the other hand, the uncertainty of the coil radius is dominated by the mechanical tolerances and therefore is much more difficult to control. The most critical components are the bearings that define the rotation axis of the coil; absolute tolerances are typically of the order of 100  $\mu\text{m}$ , and this figure can be substantially reduced only by taking rather expensive measures (e.g. ceramic coil supports and ball bearings). As a result, we find typically relative uncertainties of the order of a few  $10^{-3}$  for quadrupole measured with rotating coils up to a few 10 mm in radius,

however this estimate will diverge rapidly when measuring high harmonic orders with smaller-diameter coils.

In addition we must consider that, at low aperture sizes, the room available to add turns to a coil is reduced. Assuming a constant peak field level at the pole tip as dictated by the magnet technology used (typically around 1 T for traditional resistive magnets, up to 9 T for NbTi superconducting magnets) as well as constant coil rotation speed (~60 rpm), we will have that available signal levels scale with the cross-sectional area available i.e. with  $R_c^2$ . In conclusion, the signal-to-noise ratio of rotating coil measurements can be expected to scale as  $R_c^3$ , which explains the challenge of the present test campaign.

### 3. COIL MANUFACTURING CHALLENGES

The accuracy of magnetic measurements with rotating coils is essentially based on the knowledge of  $A_c$  and  $R_c$ . Winding techniques with copper wires allow typically to achieve coil areas within 1% of the design value. After careful calibration, shafts can be equipped with sets of coils hand-picked from large production series having identical areas within a few  $10^{-4}$ . The high packing density than can be achieved with small wires (at CERN, the smallest practical wire diameter in current use is about 30  $\mu\text{m}$ , excluding insulation) allows relatively large effective areas even in small coils. On the other hand, one must produce 3 to 5 times more coils than needed for a given array in order to find a sufficient number of coils within the required accuracy. In addition, the smaller the coil geometry, the more difficult is the precise machining of the coil cores.

The problem is different when producing coils with PCB techniques. In this case, we superpose up to 20-single or double 30 layers on which a number of spiral tracks was printed. The number of turns per layer is defined by the available space. Track width and insulation gaps can go down to 50  $\mu\text{m}$  for small geometries. The coil must be designed in a way that finally all layers can be connected in series with metallized holes drilled in the compressed stack of layers. The packing density is approximately 6 times lower than for classic winding with wires. The coil length is commonly limited to about 500 mm; larger sizes up to about 1.3 m are possible, but this requires special equipment that very few firms on the market possess. The main issue is precise superposition of the layers. In addition, the PCB coils must be carefully cut out of the stack in a way that it can then be precisely located with respect to an external reference. On the other hand, PCB coils show a reproducibility of the effective coil areas of the order of  $10^{-4}$ , so very well-matched arrays can be printed efficiently on the same layer.

### 4. CALIBRATION OF $\varnothing 8$ MM SYSTEM

In this section we present the results of the calibration of the two  $\varnothing 8$  mm systems fabricated, identified as CLIC01 (in use now at PSI) and CLIC02 (in use at CERN). Whenever possible, so-called in-situ calibrations have been carried out with reference magnets of different lengths so as to obtain

the average of geometric parameters over different parts of the coil, weighted with the longitudinal field profile of the target magnet [10]. In all cases, the rotating shaft was centred longitudinally with respect to the reference magnet. The values referred to as taken over the full length of the coil (150 mm in this case) were obtained instead from a standard calibration inside a large-size dipole and quadrupole providing a uniform and known field and gradient, respectively, over about 1.5 m length. Such calibration, which is routinely performed for every coil built, provides the global arithmetic average of the coil parameters.

#### 4.1. Calibration at CERN

In Tables 2 and 3 we list the calibrated parameters of the CLIC01 and CLIC02 shafts. The comparison between the two coil shafts is relevant to verify the reproducibility of the PCB fabrication technique, which is expected to be rather high.

TABLE 2. PARAMETERS OF CLIC01  $\varnothing 8$  MM SHAFT  
VALUES OBTAINED AT CERN AND AT PSI (*IN ITALICS*)

Coil	A	B	C
Length (mm)	150	150	150
Number of turns	200	200	200
$R_c$ over 150 mm (mm)	2.750	0.464	1.069
$R_c$ over 80 mm (mm)	2.768	0.822	2.342
$A_c$ over 150 mm (mm <sup>2</sup> )	66.520	163.170	96.700
$A_c$ over 80 mm (mm <sup>2</sup> )	66.201	163.000	96.500

TABLE 3. PARAMETERS OF CLIC02  $\varnothing 8$  MM SHAFT  
VALUES OBTAINED AT CERN

Coil	A	B	C
Length (mm)	150	150	150
Number of turns	200	200	200
$R_c$ over 150 mm (mm)	2.662	0.309	1.255
$R_c$ over 45 mm (mm)	2.679	0.336	1.236
$A_c$ over 150 mm (mm <sup>2</sup> )	66.500	163.110	96.670
$A_c$ over 45 mm (mm <sup>2</sup> )	66.203	163.575	96.073

The measured difference between the total effective areas of the two shafts is in fact only  $3 \cdot 10^{-4}$ , averaged over the three coils. This difference is very small and represents a marked improvement over the traditional winding technique. The average effective surface difference as a function of the length of the reference magnet, on the other hand, is about  $5 \cdot 10^{-3}$ . Such a large difference is hardly consistent with the previous result and may be due to mechanical imperfections in the rotation during the in-situ calibration, such as a large sag that depends on the longitudinal compression exerted when the coil is mounted on its supports.

Considering then the rotating coil radius, both the differences between shafts and the variations as a function of reference magnet length are much higher, up to about 3% for the top and bottom coils (A and C). The differences are even higher for the central coil B, which by design should have a radius equal to zero but in reality is found to have  $R_c$  up to about 0.5 mm. Overall, these results indicate that the monolithic PCB coil assembly has originally a very good

geometrical precision, which is somewhat impaired by the subsequent machining and by the tolerances of the ball bearings (which in this case are made of plastic).

#### 4.2. Cross-check at PSI

In situ calibration of these harmonic coils was carried out using as a reference a Linac4 permanent-magnet quadrupole, qualified preliminarily at CERN with a stretched-wire system, and a reference QFF quadrupole. Both magnets have an 80 mm long yoke and hence, approximately, the same longitudinal gradient profile. The integrated field gradient obtained during the measurements of some QFF prototypes was then double-checked at PSI using a system of three AREPOC LHP-MU Hall probes, built for this purpose. The simultaneous field measurement of the two probes with a constant space in between, allows correcting the position errors coming from the magnet misalignment and from the vibration of the Hall probe arm. The rotating coils show excellent reproducibility, expressed as the r.m.s calculated over ten measurements repeated in the same conditions. The precision of integrated field strength and harmonic measurement is 1 unit and 0.1 units at a radius of 3 mm, respectively. Systematic errors of 0.5 % were corrected using Hall probe measurements. As an illustration, Fig. 4 displays the variation of the transfer function with the current for QFF(P2) measured with the CLIC01  $\varnothing$ 8 mm rotating coils and cross-checked by the Hall probe.

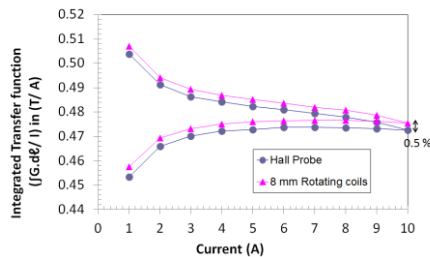


Fig. 4 - Variation of the transfer function (in T/A) of the current measured with the  $\varnothing$ -8 rotating coils and a Hall probe

### 5. CALIBRATION OF $\varnothing$ 19 MM SYSTEM

#### 5.1. Calibration at CERN

The results of the calibration of the two existing  $\varnothing$ 19 mm  $\times$  400 mm systems, identified as L401 (now at PSI) and L402 (in use at CERN) are presented in Tables 4 and 5.

TABLE 4. PARAMETERS OF L401  $\varnothing$ 19 MM SHAFT VALUES OBTAINED AT CERN AND AT PSI (IN ITALICS)

Coil	A	B	C
Length (mm)	400	400	400
Number of turns	100	64	64
$R_c$ over 400 mm (mm)	6.940	0.121	5.684
$R_c$ over 150 mm (mm)	7.036	0.036	5.599
$A_c$ over 400 (m <sup>2</sup> )	0.2055	0.4531	0.2223
$A_c$ over 150 (m <sup>2</sup> )	0.2055	0.4531	0.2223

TABLE 5. PARAMETERS OF L402  $\varnothing$ 19 MM SHAFT VALUES OBTAINED AT CERN

Coil	A	B	C
Length (mm)	400	400	400
Number of turns	100	64	64
$R_c$ over 400 mm (mm)	7.033	0.020	5.559
$R_c$ over 180 mm (mm)	6.957	0.060	5.596
$A_c$ over 400 (m <sup>2</sup> )	0.1883	0.4523	0.2538
$A_c$ over 180 (m <sup>2</sup> )	0.1887	0.4532	0.2542

#### 5.2. Cross-check at PSI

The integrated field gradient obtained during rotating coils measurements of the four QFD prototypes was systematically double-checked using a system of three Hoeben HE-244 Hall probes, built for this purpose. As for the QFF, the magnetic field measurements with the Hoeben probes were performed with the two current polarities to correct background field errors. The  $\varnothing$ 19 mm coils show almost the same excellent reproducibility as the  $\varnothing$ 8 ones (1 unit for the integrated field strength and 0.2 units for the harmonics at a radius of 8 mm). The cross-check highlights a difference up to 0.3 % with the rotating coils (Fig. 5).

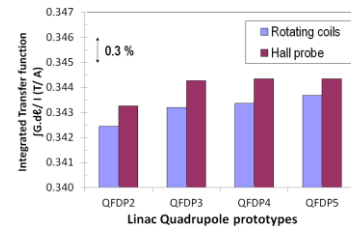


Fig. 5 - Difference in the transfer function (in T/A) measured with the  $\varnothing$ -19 rotating coils and the Hall probe

### 6. SERIES QUADRUPOLES TEST RESULTS

The magnetic tests for the SwissFEL series quadrupoles are mainly based on rotating coil measurements. The integrated field gradient, the roll angle, the multipole content and the effect of the steerers cycling on the quadrupole magnetic axis are measured in reproducible conditions at room temperature. The pre-cycling conditions consist of three current cycles between -10 A and +10 A. As an illustration, Figs. 6a and 6b show two types of measurements performed at PSI using the 19 mm shaft:

- the quadrupole strength as a function of the current expressed using the transfer function,  $TF = \int Gd\ell/I$  where  $I$  is the excitation current, measured on 65 QFD magnets (Figs. 6 a)
- the distribution of the roll angle obtained by measuring the skew quadrupole component  $a_2$  of the same QFD quadrupoles (Fig. 6b). To cancel out the systematic error from the misalignment between the encoder axis of the rotating shaft and the axis of the quadrupole, the harmonic measurement was carried out by flipping the magnet by 180° around the vertical axis. The random errors (1  $\sigma$  rms) resulting from a minimum of three consecutive measurements is ranging up to 0.1 mrad.

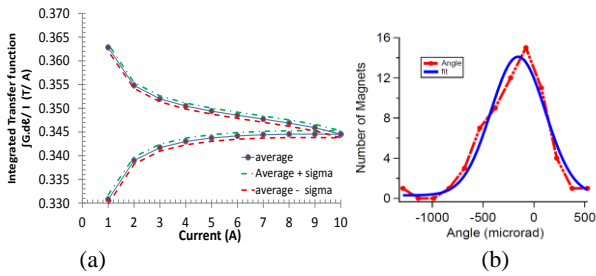


Fig. 6a - Integrated transfer function in T/A as a function of the current measured for 65 QFD quadrupoles. The average values and the boundaries limited by the average  $\pm 1 \sigma$  are presented. Fig. 6b - Distribution of the field roll angle (expressed in  $\mu\text{rad}$ ). The experimental data (points) are fitted using a Gaussian distribution (line).

The  $\varnothing 8$  mm rotating coil was used for the qualification of the four QFF magnet prototypes. The 24 series magnets will be measured at PSI during summer 2014. In Fig. 7, a plot of the spectrum of the measured field harmonics at a current of 10 A is shown. The plot displays the typical pattern of harmonic contents of small aperture magnets with high values and variations of low-order harmonics like  $b_3$ ,  $a_3$ ,  $b_4$  related to the difficulties to respect the mechanical tolerances of each pole position w.r.t the other quadrants during magnet assembly.

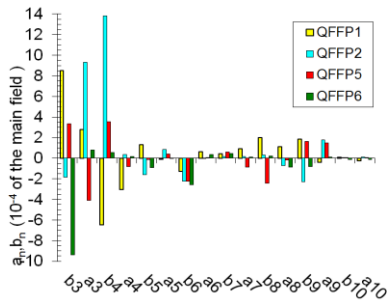


Fig. 7 - Integrated normalized harmonics for the 4 QFF prototypes measured at 10 A at a radius of 3 mm.

## 7. CONCLUSIONS

We have shown that careful calibration can quantify precisely the geometrical imperfections of small scale rotating coils. The in-situ calibration method has been proven to be an efficient procedure to qualify this type of magnetic measurement device by providing additional information about the variation of calibrated parameters along the coil.

By comparing the geometrical uncertainties of the two different shaft construction methods, we have observed that the PCB coils have much better reproducible effective surfaces than the monolithic version. This result is consistent with expectations, since the PCB tracks are printed with automated, micrometric precision equipment whereas more traditional coils are affected by manual winding procedures and from the uneven distribution of the epoxy glue that binds the turns together.

On the other hand, the rotating radius of the PCB assemblies has been measured to be as much as 0.5 mm off

the design value. As seen in Section 2.2, in relation to the small radii, a very careful calibration is mandatory in order to provide reasonably accurate result. We must remark that, even after calibration, the resulting mismatch between coil coefficients makes analog harmonic bucking as described above very difficult to achieve; it might be necessary then to adopt other techniques, such as separate acquisition of all coil signals and subsequent numerical bucking.

At any rate, the two systems tested appear to be adequate for the characterisation of the series quadrupoles within the tolerance required by SwissFEL. The two systems are fast, reliable and polyvalent and therefore very well adapted for series measurements. Moreover the results obtained with the 8-mm shaft manufactured in printed circuit board technology open a bright perspective in the construction of long and accurate coils to measure the field quality of the small gap aperture dipoles.

## ACKNOWLEDGMENTS

The authors wish to thank R. Beltron Mercadillo, D. Côte, L. Gaborit, D. Giloteaux, G. Golluccio and D. Oberson of the Technology Department, CERN, for their contribution to the development and manufacture of the rotating coils and the belonging acquisition systems.

## REFERENCES

- [1] S. Reiche, "Status of the SwissFEL facility at the Paul Scherrer Institut", Proc. of FEL11, pp.223-226, 2011
- [2] S. Humphries, *Principles of Charged Particle Acceleration*, Wiley, New York, 1999
- [3] S. Russenschuck, *Field Computation for Accelerator Magnets: Analytical and Numerical Methods*, Wiley, New York, 2011
- [4] S. Sanfilippo et al., "Design and magnetic performance of small aperture prototype quadrupoles for the SwissFEL at the Paul Scherrer Institut", IEEE Trans. Appl. Supercond. 24 (2014).
- [5] Arpaia, M. Buzio, O. Dunkel, D. Giloteaux, G. Golluccio, "A measurement system for fast-pulsed magnets: a case study on Linac4 at CERN", 2010 IEEE Instrumentation & Measurement Technology Conference (I2TMC), 3-6 May 2010, Austin, USA
- [6] P. Arpaia, M. Buzio, G. Golluccio, L. Walckiers, "A polyvalent harmonic coil testing method for small-aperture magnets", Rev. Sci. Instrum. 83, 085116, 2012
- [7] R. Beltron Mercadillo, R. de Oliveira, O. Dunkel, L. Gaborit, "Rotating Coil Array in "Mono-Bloc" Printed Circuit Technology for Small Scale Harmonic Measurements", IMM17, International Magnetic Measurement Workshop, La Mola, Barcelona, 18-23 September 2011
- [8] L. Walckiers, "Magnetic measurement with coils and wires", CERN Accelerator School on Magnets, Bruges, 16-25 June 2009.
- [9] M. Buzio, "Fabrication and calibration of search coils", CERN Accelerator School on Magnets, Bruges, 16-25 June 2009
- [10] P. Arpaia, M. Buzio, G. Golluccio, L. Walckiers, "In situ calibration of rotating sensor coils for magnet testing", Rev. Sci. Instrum. 2012 Jan;83(1)
- [11] ISO 5725-1, "Accuracy (trueness and precision) of measurement methods and results - Part 1: general principles and definitions"